Smart Structures and Systems, *Vol. 27, No. 5 (2021) 837-846*
DOI: https://doi.org/10.12989/sss.2021.27.5.837

Stress, sensitivity and frequency analysis of the corrugated diaphragm for different corrugation structures

Meisam Farajollahi*[1], Mehrad Goharzay [2], Daryoosh Borzuei [1] and Seyed Farhan Moosavian [1]

[1] *School of Advanced Technologies, Iran University of Science and Technology, Tehran, Iran*
[2] *School of Mechanical Engineering, Amir Kabir University of Technology, Tehran, Iran*

(*Received August 10, 2020, Revised January 2, 2021, Accepted January 25, 2021*)

Abstract. Corrugated and flat circular diaphragm-based piezoresistive pressure sensors are designed and proposed for different applications. Regarding to different criteria including maximum stress, sensitivity and natural frequency, different diaphragms with semicircular, sinusoidal and trapezoidal corrugation are modeled, simulated and investigated in finite element software. The finite element model is validated by experimental results from the literature and also with theoretical formula to ensure the accuracy of the finite element modeling process. Wavelength and location of the corrugation are optimized to achieve best performing sensor. For the application with large acceptable induced stress, circular flat diaphragm is proposed. To enhance the sensitivity of the sensor as a crucial parameter, semicircular corrugation for circular diaphragm with 360 μm wavelength and 240 μm distance from the center is designed and proposed. This configuration shows obvious improvement of the sensitivity with more than 18% enhancement. To extend the working range of the sensor regarding to input frequency, trapezoidal corrugation with 360 μm wavelength and 240 μm distance from the center is proposed to reach more than 29% enlargement in first natural frequency. Eventually, this paper tries to provide an overview to design the optimal pressure sensor according to desired specifications.

Keywords: pressure sensor; diaphragm; corrugation; sensitivity; Finite Element Analysis

1. Introduction

Technological development on microfabrication technology to build miniaturized MEMS-based devices, offers high accuracy, high sensitivity, small size and low cost sensors for different applications. Certainly, pressure sensors are one of the most common sensors with wide range of applications including automotive, gas turbine, aerospace, bioengineering, instrumentation and petroleum industries (Xu *et al*. 2016). Most typical mechanism of the pressure sensors is based on deflection of the thin flexible diaphragm as a primary element which bends due to an applied differential pressure. Different methods have been proposed to convert this deflection to measurable quantity including optical technique (Zhu *et al*. 2017), piezoresistive (Meti *et al*. 2016), piezoelectric (Ebrahimi *et al*. 2020) and capacitive (Balavalad and Sheeparamatti 2015).

Since the development of MEMS technology, piezoresistive diaphragm-based pressure transducers have become the dominant types and maintain their share of the industrial field, due to their stability, high performance, low cost, ease of fabrication, stability, linearity and repeatability (Tran *et al*. 2018). But in some cases including high temperature applications, the capacitive type is preferred because of its high performance and high sensitivity and also less sensitivity to temperature variation (Balavalad and Sheeparamatti 2015). Piezoresistive pressure sensors utilize the piezoresistive materials to capture the strain or deflection induced by applied pressure and convert it to detectable voltage using electrical circuit. Performance enhancement of this kind of sensors, have gained large number of research and studies to improve their sensitivity, range and accuracy by changing geometry, shape, material and configuration (Zhao *et al*. 2016).

Diaphragm's shape is one of the effective variables which has been investigated by different researchers to find the best shape regarding to maximum tolerable stress, maximum deflection and best sensitivity (Nallathambi and Shanmuganantham 2015b, Suja *et al*. 2013). Some of the results show that in the same condition, circle has less stress and larger deflection which is suitable for sensitivity compare to square and rectangle (Fathi and Moradi 2014). Suja *et al*. (2013) investigated three different shapes and they showed that the circular shape has the better performance but due to the limitations in VLSI manufacturing, they preferred to work on square shape. They also used silicon and SOI materials for their simulations and compare the results and obtained that these two different materials have different behaviors under various range of applied pressure.

In another work, the cross-beam piezoresistive pressure sensor with the aluminum beam was developed and showed that this structure could enhance the sensitivity of the sensor and reached 3.8 times higher than the flat membrane (Yu and Huang 2015).

*Corresponding author, Ph.D.,
E-mail: farajollahi@iust.ac.ir

ISSN: 1738-1584 (Print), 1738-1991 (Online)

The maximum deflection at the center of three different shapes for environmental application was investigated and regarding to applied environmental pressure, the different sensitivities were observed (Nallathambi and Shanmuganantham 2015b). In the range of environmental pressure, square shape which had larger deflection, smaller stress and also smaller difference between theoretical formula and FEM simulation has been proposed.

Graphene based rectangular diaphragm with different dimensions and thicknesses were analyzed and observed that the stress is directly related to the thickness of the diaphragm but the effect of thickness is less significant when thickness decreases to 0.25 μm with length/width ratio of 6. It was shown that this diaphragm is very sensitive to applied pressure and is suitable for applications in miniaturized highly sensitive pressure (Rahman *et al*. 2017).

In another research, silicon carbide has been used as a material for circular piezoresistive diaphragm and good linearity and sensitivity at the center of the circle was achieved. In this paper, silicon carbide exhibit 13% better sensitivity in comparison with silicon made diaphragm (Shaklya *et al*. 2018).

Several materials have been selected and proposed to make diaphragm based pressure sensors including polycrystalline silicon (Mosser *et al*. 1991), Graphene (Zhu *et al*. 2013), SOI substrate with Oxygen ion implantation (Li *et al*. 2012) Germanium (Shaby *et al*. 2015), Parylene (Luharuka *et al*. 2006), Silicon nanowires (Lou *et al*. 2012) and each material and proposed structure has its own advantages and drawbacks.

Diaphragm made of different materials such as diamond thin film (DTF) and poly-silicon were investigated and some important parameters including stress, deflection and sensitivity were studied. The finite element simulation using COMSOL showed that the cantilever made of DTF had higher sensitivity compare to poly-silicon one (Mathur *et al*. 2017).

Configuration as a third important and effective variable also has gained many attentions. Thanks to microfabrication progress, different configurations such as corrugated structure is increasingly considered to enhance the performance of the diaphragm based pressure sensors. Corrugated diaphragms (CDs) have been extensively implemented due to wider linear range and higher pressure sensitivity compared to flat diaphragms (Ganji and Taybi 2017, Li *et al*. 2019).

Gui *et al*. (2016) observed effective improvement in sensitivity of the circular diaphragm using corrugated structure. They reached 0.44 μm/MPa which is two times larger than the same size planar diaphragm.

A diaphragms with planar and corrugated shapes under thermal and load-deflection were analyzed. The proposed corrugated diaphragm was made of Parylene and the effect of the corrugation depth and corrugation number on mechanical sensitivity was investigated parametrically. In the finite element study, it was observed that corrugated structure significantly reduces the residual stress and also increases the deflection more than 5 times in comparison with flat diaphragm (Sim *et al*. 2005).

For applications to micromachined high-sensitivity devices such as microphones and pressure sensors, single deeply corrugated diaphragm with different initial stresses and corrugation depths has been studied. The FEM and theoretical analysis showed that the significant enhancement in sensitivity is achieved by corrugated diaphragm with deep corrugation. The measurement results were in good consistency with FEM and theoretical results (Wang *et al*. 2004).

In case of natural frequency analysis, dynamic characteristics and structural behaviors of the multilayer thin-film PZT diaphragm was studied using ANSYS FEM software and displacement and voltage response in PZT-layer at center point of the diaphragm as a function of frequency was obtained. The linear relationship between natural frequency and thickness of PZT layer was observed (Mohammadi and Sheikhi 2009).

Micromachined circular piezoelectric diaphragms made of PZT film and thermally grown silicon oxide under symmetric and asymmetric mechanical and electrical input was investigated. It was observed that however the results were in reasonable agreement with theoretical value at the first natural frequency, but in higher modes, the resonance frequencies deviate from the theoretical values because of the finite stiffness of the diaphragms (Hong *et al*. 2006).

As can be understand from the literature, the corrugated structure plays an important role in sensitivity enhancement and dynamic and structural behaviour of the diaphragm in high sensitive applications including pressure sensors and microphones. Its capability to exhibit large deflection compare to flat diaphragm, causes smaller induced stress and also wider input range which attracts researchers to work on this kind of diaphragm. Regarding to improvement in performance and sensitivity of the sensor and to design an optimal diaphragm depends on various applications and environments, the effect of the geometrical and configurational parameters of the corrugation on stress, sensitivity and natural frequency are studied and investigated in this paper. The results can help one to design a high sensitive and efficient diaphragm-based pressure sensor.

Depends on the different applications and criteria, best performance pressure sensor is designed and proposed. Finite element analysis using ABAQUS software has been applied to find the optimal variables (wavelength and location of the corrugation) for three different corrugations. Smaller induced stress, better sensitivity and larger natural frequency have been selected as design criteria to investigate the results and compare them to find the best performance.

2. Principle of operation

The primary function of the diaphragm as an elementary element, is to convert the applied pressure to a measurable and physical variable which is deflection. The mechanical deformation which causes mechanical strain, induces stress in the piezoresistive sensors. The piezoresistive sensors or

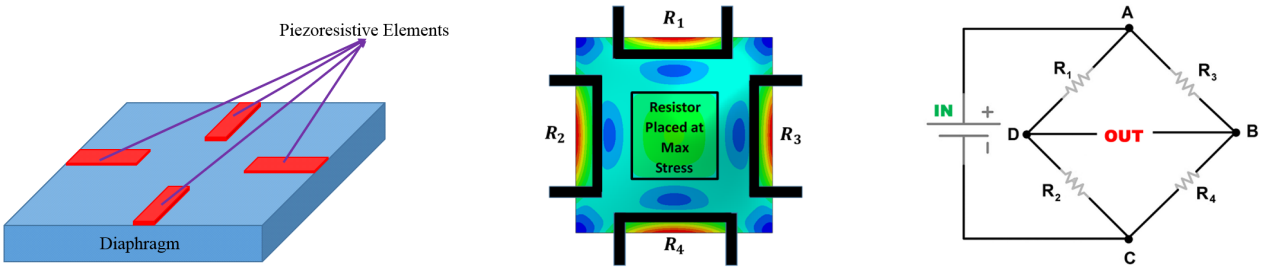

(a) (b) (c)

Fig. 1 Schematic of the arrangement of the four piezoresistive elements and the used Wheatstone bridge circuit: (a) 3D view; (b) top view; (c) Wheatstone bridge circuit

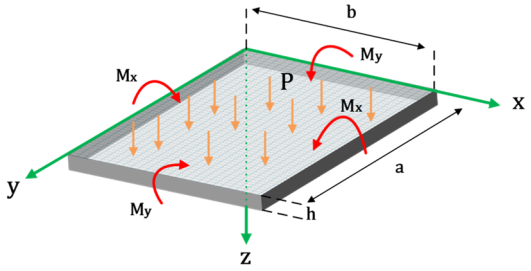

Fig. 2 A Diaphragm under distributed uniform pressure

strain gages used as a secondary elements, are the sensors which their resistivity changes as a function of the induced stress. The resistivity variation is detected by designed electrical circuit. This circuit converts this resistance change to output voltage when the circuit is driven by constant current source. The piezoresistive sensors are made of metal or semiconductor which their resistivity change as a function of applied stress and when the constant applied current is applied, the output voltage changes due to the change in the final resistance. This resistivity change is directional and depends on the material structure.

3. Mathematical modeling and governing equations

When the diaphragm is subjected to differential pressure between its two sides, diaphragm starts to deflect due to the bending moment created by pressure difference. This bending moment is applied because the circumference of the diaphragm is clamped and the distributed pressure plays a bending moment on the diaphragm and causes tension or compression inside the diaphragm.

When the clamped diaphragm is under uniform pressure as shown in Fig. 2, there are two sources of stress:

- Normal stresses (σ_{xx} and σ_{yy}) which cause bending moments (M_x and M_y)
- Shear stress (σ_{xy}) which causes torsional moment (M_{xy})

Regarding to the theory of plates, for the clamped edge diaphragm, governing differential equation to find the induced deflection ($w(x,y)$) is given by (Balavalad and Sheeparamatti 2015)

$$\left(\frac{\partial^2}{\partial x^2}+\frac{\partial^2}{\partial y^2}\right)\left(\frac{\partial^2 w}{\partial x^2}+\frac{\partial^2 w}{\partial y^2}\right)=\frac{P}{D},\quad D=\frac{Eh^3}{12(1-\nu^2)} \tag{1}$$

Where P is applied pressure, w is deflection of the plate and D is flexural rigidity of the plate. E, ν and h are Young's Modulus, Poisson's ratio and thickness of the plate respectively. Applying clamped edge boundary conditions to solve the equation 1 gives us the deflection of the plate as a function of position for the diaphragm. Knowing the diaphragm deflection and using mechanics of material formulations, lead to calculate the bending (Kaghazian *et al.* 2017, Uzum and Civalek 2019) and torsional moments and also normal and shearing stresses

$$M_x=-D\left(\frac{\partial^2 w}{\partial x^2}+\nu\frac{\partial^2 w}{\partial y^2}\right) \tag{2}$$

$$M_y=-D\left(\frac{\partial^2 w}{\partial y^2}+\nu\frac{\partial^2 w}{\partial x^2}\right) \tag{3}$$

$$M_{xy}=D(1-\nu)\frac{\partial^2 w}{\partial x\partial y} \tag{4}$$

$$(\sigma_{xx})_{max}=\frac{\sigma(M_x)_{max}}{h^2} \tag{5}$$

$$(\sigma_{yy})_{max}=\frac{\sigma(M_y)_{max}}{h^2} \tag{6}$$

$$(\sigma_{xy})_{max}=\frac{\sigma(M_{xy})_{max}}{h^2} \tag{7}$$

From the literature, the circular diaphragm in case of sensitivity and also stress reveals better behaviour compare to rectangular and square shapes with similar area and under same applied pressure (Fathi and Moradi 2014).

For circular diaphragm, the maximum stress in r and θ directions are

$$(\sigma_{max})_{rr}=\frac{3Q}{4\pi h^2},\quad Q=\pi.r^2.P, \tag{8}$$

$$(\sigma_{max})_{\theta\theta}=\frac{3\nu Q}{4\pi h^2}. \tag{9}$$

The maximum deflection of the circular diaphragm can be calculated by Zhu *et al*. (2017)

$$\frac{Pr^4}{Eh^4} = \frac{16}{3(1-\nu^2)}\left(\frac{y}{h}\right) + \frac{7-\nu}{3(1-\nu)}\left(\frac{y}{h}\right)^3, \quad (10)$$

Where h, r, E and υ are thickness, radius, Young's Modulus and Poisson's ratio of the diaphragm respectively.

In the simplified case when $y < \frac{h}{2}$, equation 10 can be modified to (Niu *et al*. 2017)

$$y = 3P \times r^4 \times \frac{1-\nu^2}{16Eh^3} \quad (11)$$

As mentioned in previous section, dynamic and frequency analysis of the diaphragm for pressure sensor application is very crucial and important. The sensor should be designed regarding to the input dynamic pressure frequency to be in the safe area and reliable distance from the natural frequency of the diaphragm to avoid resonance and probably destroying the sensor.

Natural frequency of the diaphragm, is a function of tension or in-plane stress, T, material properties including Young's Modulus, E, and density, ρ, and also diaphragm dimension (thickness, *h* and radius, *r*). Experimental results approves that it is more accurate to consider both effect of bending and in-plane stress to predict the natural frequency of the diaphragm (Malhaire 2012). Eq. (12) shows the dependency of the natural frequency to material properties and Eq. (13) to tension in the diaphragm due to in-plane stress. Eq. (14) is combination of these two parameters which gives accurate calculation of natural frequency.

$$f_{mn_{(unstress\ membrane)}} = \frac{\beta_{mn}^2}{2\pi r^2}\sqrt{\frac{Eh^3}{12\rho(1-\nu^2)}} \quad (12)$$

$$f_{mn_{(membrane)}} = \frac{\alpha_{mn}}{2\pi r}\sqrt{\frac{T}{\rho h}} \quad (13)$$

$$f_{mn}^2 = f_{mn_{(membrane)}}^2 + f_{mn_{(unstress\ membrane)}}^2 = \left[\frac{\alpha_{mn}}{2\pi r}\sqrt{\frac{T}{\rho h}}\right]^2 + \left[\frac{\beta_{mn}^2}{2\pi r^2}\sqrt{\frac{Eh^3}{12\rho(1-\nu^2)}}\right]^2 \quad (14)$$

Where α_{mn} is a constant which depends on the vibration modes and f_{mn} is the natural frequency and the subscript m and n are the number of nodal diameters and circles for the vibration mode. *E*, *v*, and ρ are Young's modulus, Poisson's ratio, and density of the material, respectively. β_{mn} is a dimensionless coefficient, and h is the membrane thickness (Hong *et al*. 2006). α_{mn} and β_{mn} are constants for circular membrane and are presented in Tables 1 and 2. T is the tension in the diaphragm but our simulation shows that there is very good consistency with FE analysis by using applied pressure instead of tension in above equation.

Table 1 α_{mn} constants for circular membrane (Malhaire 2012)

(m,n)	(0,*)	(1,*)	(2,*)	(3,*)
(*,1)	2.405	3.832	5.134	6.380
(*,2)	5.520	7.016	8.417	9.761
(*,3)	8.654	10.174	11.620	13.015
(*,4)	11.791	13.324	14.796	16.224

Table 2 β_{mn} constants for circular membrane (Malhaire 2012)

(m,n)	(0,*)	(1,*)	(2,*)	(3,*)
(*,1)	3.1962	4.6109	5.9057	7.1435
(*,2)	6.3064	7.799.	9.1969	10.5367
(*,3)	9.4395	10.9581	12.4022	13.7951
(*,4)	12.5771	14.1086	15.5795	17.0053

4. Finite element simulation and analysis

The accuracy of the FE simulation depends on several parameters including model discretization, element type, number of elements and element type. This means that the FE results should be evaluated by experiment or exact mathematical model. To ensure accurate FE simulation results, the results have been validated by the experimental results presented in Ref. (Eaton *et al*. 1999). Fig. 3 illustrates the comparison between the experimental and FE results which they are in reasonable consistency especially for smaller diameters which verifies the FE simulation process. Now, the FE simulation can be continued to model the further and more complex cases.

As mentioned before, the circular shape in case of sensitivity and stress, is more efficient comparing to square and rectangular one, so, in this paper, the circular diaphragm has been selected to design the high sensitive pressure sensor. Silicon also has been selected as a material for diaphragm which is one of the best option regarding to literature results and reports (Nallathambi and Shanmuganantham 2015a, Fathi and Moradi 2014, Niu *et al*. 2017a). The properties of the silicon-based diaphragm are presented in Table 3. All degree of freedoms of the nodes at circumference of the diaphragm were constrained to model the fully clamped configuration and uniform distributed external pressure was applied.

The FE simulation results were compared also with theoretical formula for maximum Von misses stress, maximum deflection and first natural frequency.

The results were in very good agreement (less than 5% error) and are illustrated in Simple circular membrane, is modeled by 3D shell with more than 42000 S4 elements and corrugated membrane is modeled by 3D shell with more than 48000 S4 elements.

Since the number of elements is not too high and the simulation is not too time consuming, it was preferred to use 3D modeling and simulation. As a boundary condition, all degrees of freedom of the elements around the

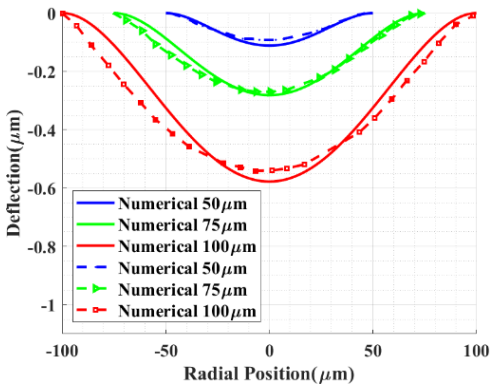

Fig. 3 Comparison among the FE results and experimental data from Ref (Eaton *et al*. 1999). The diaphragm was made of silicon nitride with 50, 75 and 100 μm radius, 1.4 μm thickness, 300 GPa Young's Modulus and 0.24 Poisson's ratio under 12 psi external pressure

Table 3 The Properties of the circular silicon diaphragm

Material	Silicon
Configuration	Circular
Young's modulus (GPa)	160
Poisson's Ration	0.22
Radius (μm)	900
Thickness (μm)	90
Density (kg/m^3)	2330

Table 4 FE simulations and theoretical results for maximum Von misses stress, maximum deflection and first natural frequency of the circular diaphragm under 5 MPa applied pressure

Maximum Von Misses Stress (MPa)		Maximum Deflection (μm)		First Natural Frequency (Hz)	
Finite element	Theory	Finite element	Theory	Finite element	Theory
333.20	341.31	4.94	5.02	4.45E+05	4.68E+05
Error = 2.38%		Error = 1.58%		Error = 4.86%	

membrane are clamped and then the load is applied perpendicularly.

Simple circular membrane, is modeled by 3D shell with more than 42000 S4 elements and corrugated membrane is modeled by 3D shell with more than 48000 S4 elements.

Since the number of elements is not too high and the simulation is not too time consuming, it was preferred to use 3D modeling and simulation. As a boundary condition, all degrees of freedom of the elements around the membrane are clamped and then the load is applied perpendicularly.

Few shapes for corrugation have been proposed in the literature including semicircle (Gui *et al*. 2016), trapezoidal (Li *et al*. 2001, Miao *et al*. 2002) and square or rectangular (Luharuka *et al*. 2006). Moreover, number and depth of the

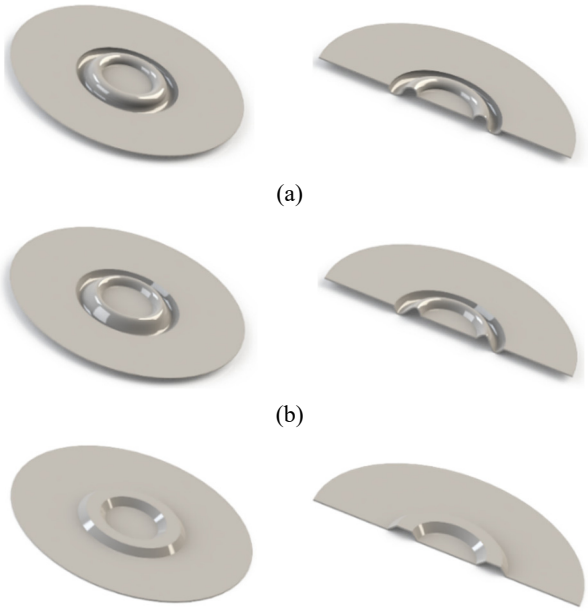

(a)

(b)

(c)

Fig. 4 Schematic of three different 1-corrugation (a) circular; (b) sinusoidal; (c) trapezoidal

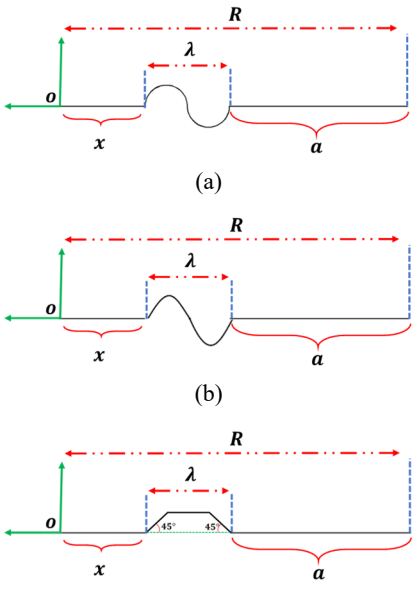

(a)

(b)

(c)

Fig. 5 Schematic half of cross-section of the corrugated circular diaphragm for (a) semicircle; (b) sinusoidal; (c) trapezoidal corrugation

corrugation are two important parameters in design and analysis that should be considered.

In this work, the semicircle, sinusoidal and trapezoidal corrugation for circular diaphragm are modeled and investigated to find the optimal and efficient design regarding to three crucial parameters including stress, deflection and sensitivity. These three corrugations are illustrated in Fig. 4.

One interesting solution to address the sensitivity enhancement (Li *et al*. 2001, Miao *et al*. 2002) and stress

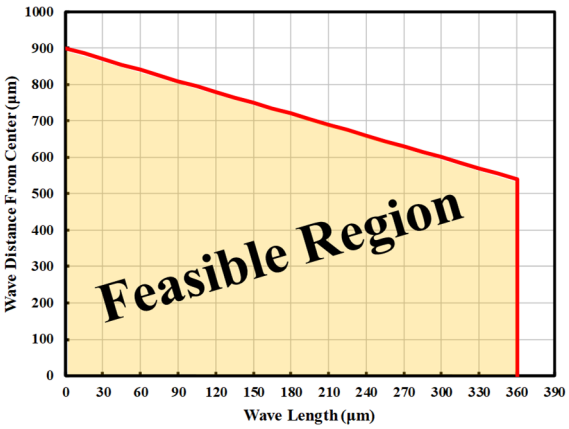

Fig. 6 Feasible region to design a corrugated circular diaphragm

issue (Ke *et al*. 2009) in diaphragm-based pressure sensors is applying corrugation configuration.

Some variables are defined to determine the configuration of the corrugated diaphragm which are radius of the diaphragm, R, distance of the initial point of the corrugation from the center, x, length of the corrugation or wavelength, λ, and distance of the end of corrugation to the circumference, a. These variables are represented in Fig. 5. The radius of the diaphragm is set to 900 μm. To discover the optimal values for stated variables, the wavelength varies between 0 and 360 μm and $\boldsymbol{x}$ between 0 and 900 μm.

Based on introduced variables, it is possible to define the feasible region as shown in Fig. 6.

5. Results and discussion

This section deals with finite element simulation results of three different types of corrugated diaphragm under external pressure and discussion of the influence of wavelength and placement of corrugation (λ and x) on defined design criteria (stress, deflection and sensitivity).

In the presented simulations, the applied pressure is 5 MPa and the diaphragm has only one corrugation but at different place along the radius of the diaphragm and varying wavelength. Three types of corrugated structures including trapezoidal, sinusoidal and semicircular are modeled and investigated.

5.1 Maximum stress analysis

It is desired that a diaphragm under given external pressure exhibits smaller stress. This means that the film can tolerate larger applied pressure, or the film with smaller maximum stress reach fracture stress in a larger applied pressure and this means wider range in input pressure.

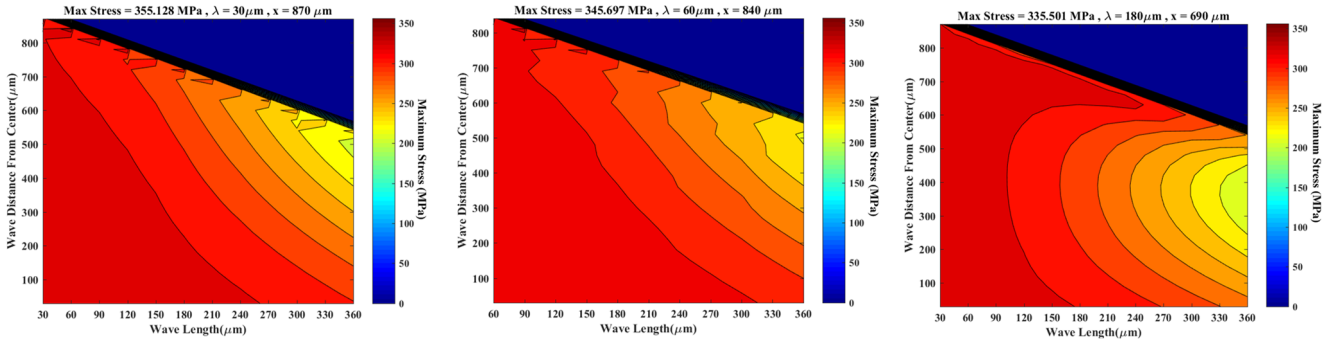

(a) Semicircle (b) Sinusoidal (c) Trapezoidal

Fig. 7 Maximum stress contour as a function of wavelength (λ) and distance from the center of the film (x) for (a) semicircle; (b) sinusoidal; and (c) trapezoidal corrugated diaphragm

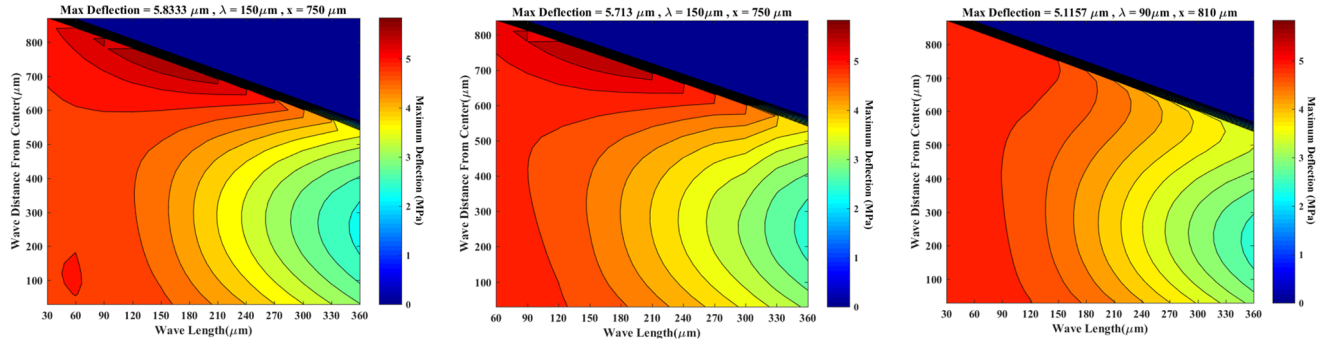

(a) Semicircle (b) Sinusoidal (c) Trapezoidal

Fig. 8 Maximum deflection contour as a function of wavelength (λ) and distance from the center of the film (x) for (a) semicircle; (b) sinusoidal; and (c) trapezoidal corrugated diaphragm

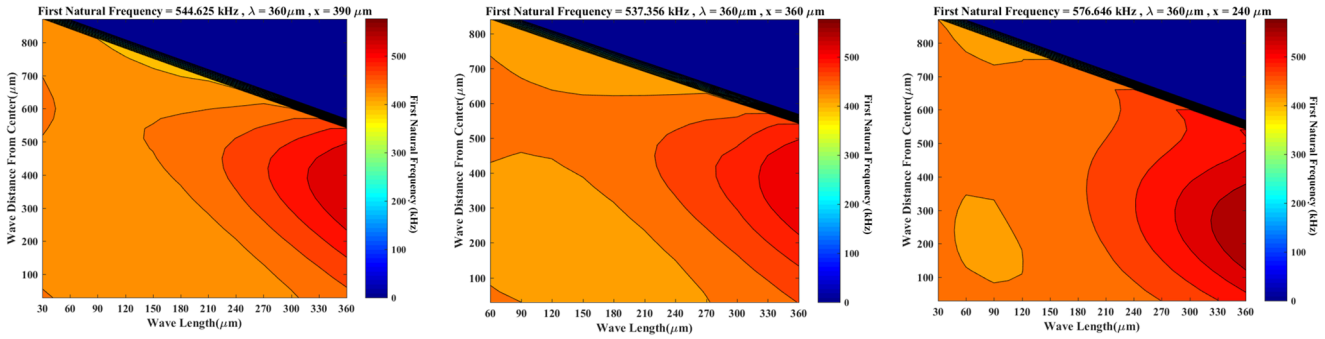

(a) Semicircle (b) Sinusoidal (c) Trapezoidal

Fig. 9 First natural frequency contour as a function of wavelength (λ) and distance from the center of the film (x) for (a) semicircle; (b) sinusoidal and (c) trapezoidal corrugated diaphragm.

Fig. 7 depicts the maximum stress contour as a function of wavelength (λ) and distance from the center of the film (x) for semicircle, sinusoidal and trapezoidal corrugated diaphragm.

As can be observed from the Fig. 7, the maximum stress under similar applied external pressure (5 MPa), occurs in the semicircular corrugation and the minimum stress in trapezoidal one. At trapezoidal corrugated diaphragm, the maximum stress happens at $\lambda = 180\ \mu m,\ x = 690\ \mu m$ with the 335.5 MPa stress. This value is 345.697 MPa and 355.128 MPa for sinusoidal and semicircular corrugation respectively.

Regarding to maximum stress criteria, trapezoidal corrugation is more optimal and efficient compare to semicircular and sinusoidal. Also, the sinusoidal has better performance in comparison with semicircular one.

Interestingly, the stress contour behavior of the trapezoidal is different compare to other two contours. For all cases, at the constant distance from the center (x), increasing the wavelength leads to decrease in stress and it is more obvious by enlarging the x.

5.2 *Sensitivity analysis*

Sensitivity is one of the important parameters to evaluate the performance of the pressure sensor and defined as a ratio of diaphragm deflection as an output with respect to unit change in applied pressure as an input. In piezoresistive sensors, this deflection causes strain which are converted to change in current or voltage due to resistance variation. High sensitive pressure sensors are required for several applications including biomedical, automobile and aviation (Zhao *et al*. 2016). Large number of papers have been published try to improve the sensitivity using different, structures, materials, configurations, dimensions and designs. It has been also experimentally confirmed that for the piezoresistive pressure sensor, using corrugated diaphragm due to its higher flexibility can improve the sensitivity by increasing deflection (Suzuki *et al*. 2019).

In this section, the maximum deflection as a function of wavelength and distance from the center has been analyzed.

Maximum deflection contour as a function of wavelength (λ) and distance from the center of the film (x) for semicircle, sinusoidal and trapezoidal corrugated diaphragm are illustrated in Fig. 8.

The maximum deflection is observed in semicircular corrugated diaphragm which is 5.833 μm at $\lambda = 150\ \mu m,\ x = 750\ \mu m$ compare to sinusoidal (5.713 μm) and trapezoidal (5.1157 μm) at the same x and λ. This means that regarding to sensitivity criteria, circular corrugated diaphragm has better performance.

At the constant x, enlarging the wavelength gives smaller deflection which is not desired.

Interestingly, for all three cases, at the many given wavelengths there are two x which have similar deflection. For instance, in case of semicircular diaphragm, at $\lambda = 240\ \mu m,\ x = 80\ \mu m$ and $x = 480\ \mu m$ have similar deflection.

Based on definition of the sensitivity $\left(\frac{Deflection}{Applied\ Pressure}\right)$ (Azqandi *et al*. 2019) and applied pressure which is fixed to 5 MPa, sensitivity has been calculated. The contour for the sensitivity has similar to maximum deflection contour just by dividing to fixed applied pressure (5 MPa).

As stated above, the sensitivity of the semicircular diaphragm at the mentioned case ($\lambda = 150\ \mu m, x = 750\ \mu m$) is 1.1667 $\frac{\mu m}{MPa}$ which is larger compare to sinusoidal (1.1426 $\frac{\mu m}{MPa}$) and trapezoidal (1.0231$\frac{\mu m}{MPa}$).

In some researches, the interesting ideas of using beam or leaf clover have been proposed to support the diaphragm to increase the sensitivity. In Hayber *et al*. (2019) 253 nm/kPa has been reached for the diaphragm with 20 μm thickness and 700 μm radius. In their research in agreement with ours, the sensitivity decrease by increasing the thickness. In another mentioned reference (Fu *et al*. 2017) 137 nm/kPa was observed for the diaphragm with 20 and 653 μm thickness and radius respectively. Both work show very large sensitivity compare to conventional clamped plates.

5.3 *Frequency analysis*

Another criteria to design a desired diaphragm, is frequency analysis. The working range of the diaphragm is a function of some parameters and one of the most important one is natural frequency. If the dynamic applied pressure frequency approaches the natural frequency of the

Table 5 Summary of the simulations according to different criteria for three corrugated diaphragms

	Stress criteria		Sensitivity criteria				Frequency criteria	
Type of corrugated	**Stress (MPa)**		**Max deflection (μm)**		**Sensitivity (μm/MPa)**		**First natural frequency (kHz)**	
Semicircular	**355.128**		**5.833**		**1.1667**		**544.625**	
	$x = 870\ \mu m$	$\lambda = 30\ \mu m$	$x = 750\ \mu m$	$\lambda = 150\ \mu m$	$x = 750\ \mu m$	$\lambda = 150\ \mu m$	$x = 390\ \mu m$	$\lambda = 360\ \mu m$
Sinusoidal	**345.697**		**5.713**		**1.1426**		**537.356**	
	$x = 840\ \mu m$	$\lambda = 60\ \mu m$	$x = 750\ \mu m$	$\lambda = 150\ \mu m$	$x = 750\ \mu m$	$\lambda = 150\ \mu m$	$x = 360\ \mu m$	$\lambda = 360\ \mu m$
Trapezoidal	**335.501**		**5.116**		**1.0231**		**576.646**	
	$x = 690\ \mu m$	$\lambda = 1800\ \mu m$	$x = 810\ \mu m$	$\lambda = 90\ \mu m$	$x = 810\ \mu m$	$\lambda = 90\ \mu m$	$x = 240\ \mu m$	$\lambda = 360\ \mu m$
Flat	**333.20**		**4.94**		**0.988**		**445.357**	

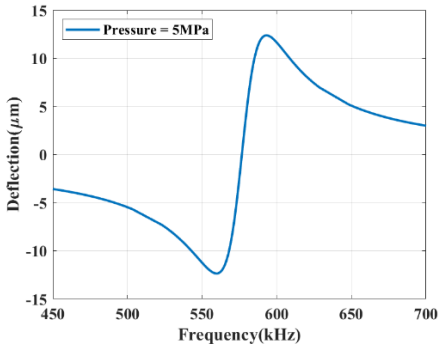

Fig. 10 Deflection versus frequency of the trapezoidal corrugated diaphragm

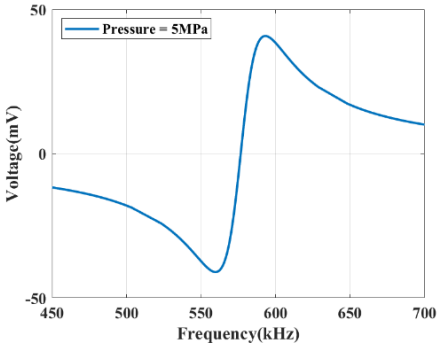

Fig. 11 Output voltage versus frequency of the trapezoidal corrugated diaphragm

diaphragm, resonance can happen and causes damage on the film due to the deflection enlargement.

Regarding to using Wheatstone bridge configuration to capture the change in voltage due to applied pressure and stress, output voltage can be calculated. The output voltage is linearly proportional to input voltage which is 5 Volts in our simulation. Equation 15 shows this relationship (Zhu *et al*. 2013).

$$V_{out} = \frac{\frac{\Delta R}{R}}{2 + \frac{\Delta R}{R}} V_{in}. \quad (15)$$

Change in resistance can be written as a function of stress (σ) and piezoresistive coefficient (π) (Niu *et al*. 2017).

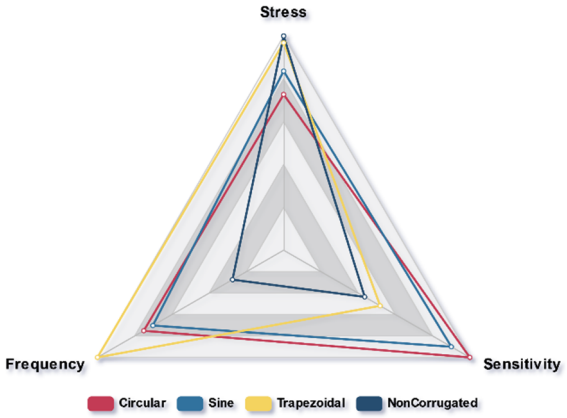

Fig. 12 Graphical representation of the results presented in Table 5

$$\frac{\Delta R}{R} = \pi_l \sigma_l + \pi_t \sigma_t, \quad (16)$$

where subscripts l and t represent transverse and longitudinal direction.

5.4 Summary

In large number of FE simulations, three different corrugated diaphragm regarding to different criteria, maximum stress, sensitivity and first natural frequency have been investigated. Each diaphragm has its own advantage based on defined criteria. Depends on application and limitations, designers can utilize one of these type of structures. Also, wavelength and location of the corrugation are two important variables which help to design high performance sensor. The simulations have been summarized in Table 5 and graphically in Fig. 12.

The fabrication techniques of the corrugated diaphragms, have been discussed in (Scheeper *et al*. 1994, Sim *et al*. 2001, Wang *et al*. 2004). Lithography, low pressure chemical vapor deposition (LPCVD), reactive ion etching and also dry etching are some important steps of fabrication process.

6. Conclusions

In this work, three different corrugated circular

diaphragms were designed and analyzed regarding to some criteria; maximum stress, sensitivity and higher natural frequency. Wavelength, λ, and location of the corrugation, x, have been defined as two important variables which play crucial roles on diaphragm functionality and performance. Finite element model was validated by experimental results from the literature and also with theory to confirm the correction process of the modeling and simulation in ABAQUS software.

For the application with requirement of large acceptable induced stress, corrugation does not have any advantageous versus flat circular diaphragm. Since the induced stress is smaller in flat diaphragm at similar condition compare to corrugated one, circular flat diaphragm pressure sensor is proposed for this specific application.

Regarding to sensitivity which has large number of applications in industry, best sensitivity was observed in semicircular corrugation at $\lambda = 150\ \mu m$ and $x = 750\ \mu m$ with more than 18% improvement in comparison with flat diaphragm. This semicircular corrugated circular diaphragm is offered for high sensitivity applications.

Trapezoidal corrugation with $\lambda = 360\ \mu m$ and $x = 240\ \mu m$ was designed to increase the first natural frequency of the diaphragm to extend the working range and make it suitable for high input frequency applications. More than 29% enlargement in first natural frequency was observed in this proposed structure.

References

Azqandi, M.S., Hassanzadeh, M. and Arjmand, M. (2019), "Sensitivity analysis based on complex variables in FEM for linear structures", *Adv. Computat. Des., Int. J.*, **4**(1), 15-32. https://doi.org/10.12989/acd.2019.4.1.015

Balavalad, K.B. and Sheeparamatti, B.G. (2015), "A critical review of MEMS capacitive pressure sensors", *Sensors Transducers*, **187**(4), 120-128.

Eaton, W.P., Bitsie, F., Smith, J.H. and Plummer, D.W. (1999), "A new analytical solution for diaphragm deflection and its application to a surface-micromachined pressure sensor", *Proceedings of International Conference on Modeling and Simulation of Microsystems*.

Ebrahimi, F., Hosseini, S.H.S. and Singhal, A. (2020), "A comprehensive review on the modeling of smart piezoelectric nanostructures", *Struct. Eng. Mech., Int. J.*, **74**(5), 559-581. https://doi.org/10.12989/sem.2020.74.5.559

Fathi, N.A. and Moradi, Z.A. (2014), "Design and Optimization of Piezoresistive MEMS Pressure Sensors Using ABAQUS", *Middle-East J. Scientif. Res.*, **21**(12), 2299-2305.

Fu, C., Si, W., Li, H., Li, D., Yuan, P. and Yu, Y. (2017), "A novel high-performance beam-supported membrane structure with enhanced design flexibility for partial discharge detection", *Sensors*, **17**(3), 593. https://doi.org/10.3390/s17030593

Ganji, B.A. and Taybi, M. (2017), "A Novel High Sensitivity MEMS Acoustic Sensor using Corrugated Diaphragm", *Majlesi J. Electr. Eng.*, **11**(4), 53-57.

Gui, Y., Zhang, Y., Liu, G., Hao, Y. and Gao, C. (2016), "Design and simulation of corrugated diaphragm applied to the MEMS fiber optic pressure sensor", *Proceedings of IEEE Annual International Conference on Nano/Micro Engineered and Molecular Systems* (*NEMS*), Sendai, Japan, December, pp. 17-20.

Hayber, S.E., Tabaru, T.E. and Saracoglu, O.G. (2019), "A novel approach based on simulation of tunable MEMS diaphragm for extrinsic Fabry–Perot sensors", *Optics Communications*, **430**, 14-23. https://doi.org/10.1016/j.optcom.2018.08.021

Hong, E., Trolier-McKinstry, S., Smith, R., Krishnaswamy, S.V. and Freidhoff, C.B. (2006), "Vibration of micromachined circular piezoelectric diaphragms", *IEEE Transactions on Ultrasonics, Ferroelectrics, and Frequency Control*, **53**(4), 697-705. https://doi.org/10.1109/TUFFC.2006.1621496

Kaghazian, A., Hajnayeb, A. and Foruzande, H. (2017), "Free vibration analysis of a piezoelectric nanobeam using nonlocal elasticity theory", *Struct. Eng. Mech., Int. J.*, **61**(5), 617-624. https://doi.org/10.12989/sem.2017.61.5.617

Ke, F., Miao, J. and Wang, Z. (2009), "A wafer-scale encapsulated RF MEMS switch with a stress-reduced corrugated diaphragm", *Sensors Actuat., A: Phys.*, **151**(2), 237-243. https://doi.org/10.1016/j.sna.2009.02.031

Li, X., Lin, R., Kek, H., Miao, J. and Zou, Q. (2001), "Sensitivity-improved silicon condenser microphone with a novel single deeply corrugated diaphragm", *Sensors Actuat. A: Phys.*, **92**, 257-262. https://doi.org/10.1016/S0924-4247(01)00582-9

Li, X., Liu, Q., Pang, S., Xu, K., Tang, H. and Sun, C. (2012), "High-temperature piezoresistive pressure sensor based on implantation of oxygen into silicon wafer", *Sensors Actuat.: A. Phys.*, **179**, 277-282. https://doi.org/10.1016/j.sna.2012.03.027

Li, H., Deng, H., Zheng, G., Shan, M., Zhong, Z. and Liu, B. (2019), "Reviews on corrugated diaphragms in miniature fiber-optic pressure sensors", *Appl. Sci.*, **9**, 2241. https://doi.org/10.3390/app9112241

Lou, L., Zhang, S., Park, W.T., Tsai, J.M., Kwong, D.L. and Lee, C. (2012), "Optimization of NEMS pressure sensors with a multilayered diaphragm using silicon nanowires as piezoresistive sensing elements", *J. Micromech. Microeng.*, **22**(5), 055012. https://doi.org/10.1088/0960-1317/22/5/055012

Luharuka, R., Noh, H.M., Kim, S.K., Mao, H., Wong, L. and Hesketh, P.J. (2006), "Improved manufacturability and characterization of a corrugated Parylene diaphragm pressure transducer", *J. Micromech. Microeng.*, **16**, 1468-1474. https://doi.org/10.1088/0960-1317/16/8/005

Malhaire, C. (2012), "Comparison of two experimental methods for the mechanical characterization of thin or thick films from the study of micromachined circular diaphragms", *Rev. Scientif. Instrum.*, **83**(5), 055008. https://doi.org/10.1063/1.4719964

Mathur, H., Agarwal, V. and Sengar, K. (2017), "Finite Element Analysis of MEMS Based Piezoresistive Diamond Thin Film Cantilever Pressure Sensor", *Int. Res. J. Eng. Technol.*, **4**(2), 1685-1689.

Meti, S., Balavald, K.B. and Sheeparmatti, B.G. (2016), "MEMS piezoresistive pressure sensor: a survey", *Int. J. Eng. Res. Applicat.*, **6**(4), 23-31.

Miao, J., Lin, R., Chen, L., Zou, Q., Lim, S.Y. and Seah, S.H. (2002), "Design Considerations in Micromachined Silicon Microphones", *Microelectr. J.*, **33**(1-2), 21-28. https://doi.org/10.1016/S0026-2692(01)00100-8

Mohammadi, V. and Sheikhi, M.H. (2009), "Design, Modeling and Optimization of a Multilayer Thin-Film Pzt Diaphragm Used in Pressure Sensor", *Int. J. Eng. Appl. Sci.*, **1**(4), 27-38.

Mosser, V., Suski, J., Goss, J. and Obermeier, E. (1991), "Piezoresistive pressure sensors based on polycrystalline silicon", *Sensors Actuat.: A. Phys.*, **28**, 113-132. https://doi.org/10.1016/0924-4247(91)85020-O

Nallathambi, A. and Shanmuganantham, T. (2015a), "Performance analysis of slotted square diaphragm for mems pressure sensor", *ICTACT J. Microelectron.*, **1**(2), 62-67. https://doi.org/10.21917/ijme.2015.0011

Nallathambi, A. and Shanmuganantham, T. (2015b), "Design of

diaphragm based MEMS pressure sensor with sensitivity analysis for environmental applications", *Sensors Transduc*., **188**(5), 48-54.

Niu, Z., Liu, K. and Wang, H. (2017), "A new method for the design of pressure sensor in hyperbaric environment", *Sensor Review*, **37**(1), 110-116. https://doi.org/10.1108/SR-04-2016-0081

Rahman, S.H.A., Soin, N. and Ibrahim, F. (2017), "Load deflection analysis of rectangular graphene diaphragm for MEMS intracranial pressure sensor applications", *Microsyst. Technol*., **24**(2), 1147-1152. https://doi.org/10.1109/84.285722

Scheeper, P.R., Olthuis, W. and Bergveld, P. (1994), "The design, fabrication, and testing of corrugated silicon nitride diaphragms", *J. Microelectromech. Syst*., **3**(1), 36-42. https://doi.org/10.1109/84.285722

Shaby, S.M., Premi, M.G. and Martin, B. (2015), "Enhancing the performance of MEMS piezoresistive pressure sensor using germanium nanowire", *Procedia Mater. Sci*., **10**, 254-262. https://doi.org/10.1016/j.mspro.2015.06.048

Shaklya, M., Magam, S.P. and Jindal, S.K. (2018), "Design, Modelling and Simulation of MEMS Piezo-Resistive Pressure Sensor with Clamped Edge Silicon Carbide Circular Diaphragm", *Proceedings of the 3rd International Conference on Internet of Things and Connected Technologies*, *ICIoTCT*, Jaipur, India, March, pp. 26-27. http://dx.doi.org/10.2139/ssrn.3170293

Sim, W., Kim, D., Kim, K., Kwon, K., Kim, B., Choi, B., Yang, S. and Park, J. (2001), "Fabrication, Test and Simulation of a Parylene Diaphragm", In: Obermeier E. (eds) *Transducers '01 Eurosensors XV*, Springer, Berlin, Heidelberg, pp. 1382-1385. https://doi.org/10.1007/978-3-642-59497-7_319

Sim, W., Kim, B., Choi, B. and Park, J.O. (2005), "Theoretical and experimental studies on the parylene diaphragms for microdevices", *Microsyst. Technol*., **11**(1), 11-15. https://doi.org/10.1007/s00542-003-0342-7

Suja, K.J., Raveendran, E.S. and Komaragiri, R. (2013), "Investigation on better sensitive silicon based MEMS pressure sensor for high pressure measurement", *Int. J. Comput. Applicat*., **72**(8), 40-47.

Suzuki, R., Nguyen, T.V., Takahata, T. and Shimoyama, I. (2019), "A Piezoresistive Vibration Sensor with Liquid on Corrugated Membrane", *Proceedings of the IEEE International Conference on Micro Electro Mechanical Systems* (*MEMS*), Seoul, Korea, January, pp. 688-691. https://doi.org/10.1109/MEMSYS.2019.8870790

Tran, A.V., Zhang, X. and Zhu, B. (2018), "Mechanical structural design of a piezoresistive pressure sensor for low-pressure measurement: a computational analysis by increases in the sensor sensitivity", *Sensors*, **18**, 1-15. https://doi.org/10.3390/s18072023

Uzun, B. and Civalek, Ö. (2019), "Free vibration analysis Silicon nanowires surrounded by elastic matrix by nonlocal finite element method", *Adv. Nano Res., Int. J*., **7**(2), 99-108. https://doi.org/10.12989/anr.2019.7.2.099

Wang, W.J., Lin, R.M. and Ren, Y. (2004), "Design and fabrication of high sensitive microphone diaphragm using deep corrugation technique", *Microsyst. Technol*., **10**(2), 142-146. https://doi.org/10.1007/s00542-003-0322-y

Xu, T., Zhao, L., Jiang, Z., Guo, X., Ding, J., Xiang, W. and Zhao, Y. (2016), "A high sensitive pressure sensor with the novel bossed diaphragm combined with peninsula-island structure", *Sensors Actuat.: A. Phys*., **244**, 66-76. https://doi.org/10.1016/j.sna.2016.04.027

Yu, H. and Huang, J. (2015), "Design and application of a high sensitivity piezoresistive pressure sensor for low pressure conditions", *Sensors*, **15**(9), 22692-22704. https://doi.org/10.3390/s150922692

Zhao, L., Xu, T., Hebibul, R., Jiang, Z., Ding, J., Peng, N., Guo, X., Xu, Y., Wang, H. and Zhao, Y. (2016), "A bossed diaphragm piezoresistive pressure sensor with a peninsula–island structure for the ultra-low-pressure range with high sensitivity", *Measure. Sci. Technol*., **27**, 1-21. https://doi.org/10.1088/0957-0233/27/12/124012

Zhu, S.E., Krishna Ghatkesar, M., Zhang, C. and Janssen, G.C.A.M. (2013), "Graphene based piezoresistive pressure sensor", *Applied Physics Letters*, **102**(16), 161904. https://doi.org/10.1063/1.4802799

Zhu, J., Wang, M., Chen, L., Ni, X. and Ni, H. (2017), "An optical fiber Fabry–Perot pressure sensor using corrugated diaphragm and angle polished fiber", *Optic. Fiber Technol*., **34**(1), 42-46. https://doi.org/10.1016/j.yofte.2016.12.004

CC